J. Condensed Matter Nucl. Sci. 28 (2019) 28–49

Research Article

Nuclear Transmutations and Stabilization of Unstable Nuclei in the Cold Fusion Phenomenon*

Hideo Kozima†

Cold Fusion Research Laboratory, Pukyung National University, Nam-gu, Yongso-ro, 45, Busan, South Korea

Abstract

We summarize the nuclear transmutations observed in the cold fusion phenomenon (CFP) putting a weight on the biotransmutation, i.e. nuclear transmutations in biological systems. The CF materials, i.e. materials where occurs the CFP, are classified into three groups: (1) the metallic material includes transition-metal hydrides (e.g. NiH_x, AuH_x) and deuterides (e.g. PdD_x, TiD_x), (2) the carbonic material includes hydrogen graphite (HC_x) and cross-linked polyethylene (XLPE) and (3) the biological material includes microorganisms, microbial cultures and biological tissues or organs. We explain these characteristics briefly in this paper. The stabilization of unstable nuclei, including the decay-time shortening of radioactive nuclei, in the nuclear transmutation is especially interesting from the applicatory point of view in relation to the treatment of the hazardous nuclear waste accompanied to the nuclear power plant. A characteristic of biological systems where occurs selective adsorption of specific ions seems especially useful for the application. If we have a microorganism or microbial culture absorbing an ion of a radioactive element selectively, we can remediate the radioactivity by the biotransmutation.
 ISSN 2227-3123

Keywords: Actinoid, Biotransmutation, Cold fusion phenomenon, Meta-analysis, Microorganism, Nuclear transmutation, Transition metal

1. Introduction

Almost 30 years have elapsed since the discovery of the cold fusion phenomenon (CFP) in PdDx by Fleischmann et al. in 1989 [1]. It should be kept in mind that hitherto we observed the CFP only in solids but not in liquids among condensed matter including a great deal of hydrogen isotopes (protium and/or deuterium). We may be able to classify the solids where the CFP (CF materials) have been observed into three groups according to the properties of host materials: (1) Metallic material including transition-metal hydrides (e.g. NiHx, AuHx) and deuterides (e.g. PdDx, TiDx). (2) Carbonic material including hydrogen graphites (HCx) and cross-linked polyethylene (XLPE). (3)

*This paper is an extended version of the paper with the same title that will be printed in *Proc. ICAMRWT (International Conference on the Application of Microorganisms for the Radioactive Waste Treatment)* (May 18, 2018, Pukyung National University, Busan, South Korea) published as a special issue of the *JCMNS* (Journal of Condensed Matter Nuclear Science).

†E-mail: hjrfq930@ybb.ne.jp.

 ISSN 2227-3123

Biological material including microorganisms, microbial cultures and biological organs. Each of the CF materials in these groups are composed of a super-lattice with a sublattice of host elements and another of hydrogen isotopes and have characteristics in the nuclear transmutations occurring there.

It should also be noted that we have observed the CFP only in these CF materials in dynamic conditions, not static conditions. This characteristic may be related to the complexity supposed to be in the CF materials ([2,3], Section 3.8).

It is also a remarkable characteristic of the CFP that there is a threshold value x of the average density of hydrogen isotopes in the CF materials for the occurrence of the CFP. The threshold value $x/X|_{\rm th}$ of the ratio x vs. X (the density of host element X) must be ≈ 0.8 or larger (in the case of transition metal hydrides and deuterides where $X =$ Ti, Ni, Pd and so forth).

These characteristics should be kept in mind when we look for the causes of the CFP based on the experimental facts obtained in this field.

It is interesting to see the ubiquitous appearance of the CFP in various CF materials as shown in Table 1.

Another characteristic of the CFP is that no gamma radiation is observed accompanying to the nuclear reactions producing transmuted nuclei, contrasting to the cases in free space where radiation such as gamma, beta and alphas are always observed.

It is natural to assume the participation of neutrons in nuclear reactions in CF materials with characteristics described above; it is common sense in nuclear physics to assume participation of neutrons to explain the occurrence of nuclear reactions in CF materials. We have proposed a model (TNCF model and its extended version, the Neutron Drop model) with an adjustable parameter to explain the cold fusion phenomenon. We have been successful to give unified systematic explanation of diverse and complex experimental data in this field [4–7].

We have deduced the existence of the trapped neutrons assumed in the TNCF model by the quantum mechanical investigation of the neutron–proton (neutron–deuteron) interaction in CF materials [7]. The justification of existence of neutrons in the CF materials composed of a superlattice of host elements and hydrogen isotopes made the TNCF model evolve into the Neutron Drop model, an extended version of the former.

Table 1. System and obtained evidence of the CFP: Host solids, agents, experimental methods, direct and indirect evidence, cumulative and dissipative observables are tabulated. Q and NT express excess energy and the nuclear transmutation, respectively. Direct evidence of nuclear reactions in the CFP are dependences of reaction products on their energy (ε) and position (***r***), decrease of decay constants of radioactive nuclides, decrease of fission threshold energy of compound nuclei.

Host solids	C, Pd, Ti, Ni, Au, Pt, KCl + LiCl, $ReBa_2Cu_3O_{7,}Na_xWO_{3,}$ KD_2PO_4TGS (triglycine sulfate), $SrCe_aY_bNB_cO_d$, XLPE (cross linked polyethylene) and biological systems (microbial cultures)
Agents	n, d, p, $^{6}_{3}$Li, $^{10}_{3}$B, $^{12}_{6}$C, $^{39}_{19}$K, $^{85}_{37}$Rb, $^{87}_{37}$Rb
Experiments	Electrolysis, liquid contact, gas discharge and gas contact
Direct evidences of nuclear reaction	Gamma ray spectrum $\gamma(\varepsilon)$, neutron energy spectrum $n(\varepsilon)$, space distribution of NT products NT(***r***), stabilization of unstable nuclei (decrease of decay constants) and lowering of fission threshold energy
Indirect evidences of nuclear reaction	Excess energy Q, number of neutrons $N_{\rm n}$, amounts of tritium atom $N_{\rm t}$, Helium-4 atom* $N_{\rm He4}$, NT products (NT_D, NT_F, NT_A), X-ray spectrum X(ε)
Cumulative observables	NT(***r***), amount of tritium atom $N_{\rm t}$, helium-4* $N_{\rm He4}$
Dissipative observables	Excess energy$Q$, neutron energy spectrum $n(\varepsilon)$, number of neutrons $N_{\rm n,}$ gamma ray spectrum $\gamma(\varepsilon)$, X-ray spectrum X(ε)

It should be noticed that CF materials include biological systems. Nuclear transmutations in them were first observed more than 200 years ago ([5],Section 10.1, [8–10]. These biological systems have been cultivated recently to include microorganisms and microbial cultures [11,12] as shown in later sections.

We have to reconsider the roles of deductive and inductive logic in science at the beginning of 21st century when we have explored new situations in science over the last 20–30 years. It should also be noted that the analysis of experimental data should be reconsidered with the meta-analysis technique, which has been used effectively in modern medical science. We give a brief overview on this problem in this paper, leaving full discussions elsewhere.

It can be said that the roots of the fruitless battle fought between people in favor of CFP and those opposed to it can be summarized as follows. (1) Persistence to the deductive logic we have been accustomed to it since the dawn of modern science in 18th century, based on the linear dynamics. (2) Ignorance of the meta-analysis that is effective to analyze complicated data observed independently in similar samples by several researchers.

Since the development of non-linear dynamics, we have to realize the fact that the cause does not determine the effect in this real world where almost all phenomena are governed by non-linear dynamics. However, this fact has almost slipped out from our discussion on the reality of the CFP in almost 30 years.

In this paper, we concentrate our discussion on the biotransmutation and its application and leave detailed discussions on other nuclear transmutations to papers and books cited in the references.

2. Experimental Results on the Nuclear Transmutation and Stabilization of Unstable Nuclei in the Cold Fusion Phenomenon

Nuclear transmutations in the cold fusion phenomenon (CFP) occur in near-surface regions of the CF materials to a depth of a few micrometers. A wide variety of nuclear transmutation products occur, and we need to classify them by some standards to investigate them scientifically.

2.1. Nuclear transmutations in the CFP

Nuclear transmutations (NTs) are classified into four kinds, according to the mechanism that produces new nuclides from the original nuclei in the CF material: nuclear transmutation by absorption ($\mathrm{NT_A}$), nuclear transmutation by decay ($\mathrm{NT_D}$), nuclear transmutation by fission ($\mathrm{NT_F}$) and nuclear transmutation by transformation ($\mathrm{NT_T}$) in our model ([6], Section 2.6), [7], Section 2.5, [13]).

The stabilization of unstable nuclei (including decay-time shortening of unstable nuclei) observed in the CFP has been successfully explained mainly by the $\mathrm{NT_D}$ mechanism, although other mechanisms are not necessarily excluded. We will explain the stabilization of unstable nuclei in this paper along the lines of the explanation in our other papers for $\mathrm{NT_D}$.

2.2. Stabilization of unstable nuclei in the CFP

We have explained the stabilization of unstable nuclei (including decay-time shortening) in the CFP as follows ([7], Section 2.5.1.1, Decay-Time Shortening).

2.2.1. *Decay-time shortening*

In general, the explanation of the mechanisms of the nuclear transmutations by decay ($\mathrm{NT_D}$) with absorption of a neutron drop ${}^{A}_{Z}\Delta$ composed of Z protons and $(A-Z)$ neutrons are given by the following reaction formulae:

$$ {}^{A}_{Z}\Delta + {}^{A'}_{Z'}X \rightarrow {}^{A-m}_{Z}\Delta + {}^{A'}_{Z'}{}^{+m}X^{*} \rightarrow {}^{A-m}_{Z}\Delta + {}^{A'+m}_{Z'+1}X' + \mathrm{e}^{-} + \underline{\nu_{\mathrm{e}}} + Q, \tag{1} $$

$$ {}^{A'+m}_{Z'}X^* \rightarrow {}^{A'+m}_{Z'+1}X' + \mathrm{e}^- + \underline{\nu_\mathrm{e}} + Q, \qquad (\beta), \tag{2} $$

$$ {}^{A'+m}_{Z'}X^* \rightarrow {}^{A'+m-4}_{Z'-2}X'' + {}^{4}_{2}\mathrm{He} + Q, \qquad (\alpha), \tag{3} $$

where α and β in parentheses designate types of the decay.

In these nuclear transmutations, there are several cases where the decay-times τ_d of the intermediate compound nuclide ${}^{A}_{Z}X^*$ in free space are very long, of the order of 10^6 –10^9 years (10^{12}–10^{15} s). The time elapsed in experiments is at most several months ($\approx 10^5$ s). Therefore, if the decay products with such long decay-times are observed, there should be drastic shortening of the decay-times (or stabilization of unstable nuclei).

The following compound nuclei correspond to this case:

$$ {}^{107}_{46}\mathrm{Pd}^* \rightarrow {}^{107}_{47}\mathrm{Ag}\,(\beta) \qquad (\tau_\mathrm{d} = 1.3 \times 10^9\,\text{years}), $$

$$ {}^{40}_{19}\mathrm{K}^* \rightarrow {}^{40}_{20}\mathrm{Ca}\,(\beta) \qquad (\tau_\mathrm{d} = \times 6.510^6\,\text{years}), $$

$$ {}^{235}_{92}\mathrm{U}^* \rightarrow {}^{231}_{90}\mathrm{Th}^*\,(\alpha) \qquad (\tau_\mathrm{d} = 1.0 \times 10^9\,\text{years}), $$

$$ {}^{238}_{92}\mathrm{U}^* \rightarrow {}^{234}_{90}\mathrm{Th}^*\,(\alpha) \qquad (\tau_\mathrm{d} = 6.5 \times 10^9\,\text{years}). $$

2.2.2. *Nuclear transmutation in actinoid hydrides and deuterides*

Experimental data sets on actinoid hydrides and deuterides prepared by electrolysis and glow discharge [14–16] have been analyzed and explained using the TNCF model [17]. The experimental data have shown that these hydrides and deuterides are classified as CF materials where CFP occur, and the observed events are understood by nuclear reactions common to other reactions observed in CF materials, mainly transition-metal hydrides and deuterides.

The changes of radiation properties of actinoids occluding hydrogen isotopes are explained by the formation of the CF-matter similar to the free neutron sea in neutron star matter [18], and then by the interaction of actinoid nucleus and the CF-matter. We have explained the experimental results [14–16] on the acceleration of the alpha decay of ${}^{238}_{92}\mathrm{U}$ into ${}^{234}_{90}\mathrm{Th}$, the so-called the decay-time shortening, by the change of the boundary layer between the nucleus ${}^{238}_{92}\mathrm{U}$ and the CF-matter. The change of the boundary layer is induced by the increase of the density ratio $n_\mathrm{o}/n_\mathrm{i}$ of neutrons (n_i and n_o are the neutron densities inside and outside the nucleus, respectively) due to the formation of the CF-matter ([19], Section 2.9).

A possible application of this phenomenon to ${}^{A}_{94}\mathrm{Pu}$ ($A = 238$–244) is hopeful.

If we can accelerate the decay of plutonium isotopes which are produced in atomic plants as hazardous waste, then it would be a tremendous help dealing with this waste, which is a serious, difficult, expensive problem. As shown in Table 2, plutonium isotopes have very long decay-times and therefore the decay-time shortening as shown in the CFP will be applicable to transmute them into other nuclides easy to treat.

Instead of neutron bombardment in free space, we can use CF-materials to produce the same effect of neutrons on target nuclei (cf. [20]). This fact may be interesting in the science and technology of neutron–nuclear interactions in the low energy region ([21], Section 3). It is a pleasant fantasy to imagine a machine that simultaneously remediates radioactive waste and generates excess energy.

Table 2. Decay characteristics of plutonium isotopes $^{A}_{94}$Pu. Decay modes, half-life (years), decay heat (W/kg) and number of spontaneous fission neutrons (per g s) are given.

Isotope	Decay mode	Half-life (years)	Decay heat (W/kg)	Spon. fission n's (1/g s)
$^{238}_{94}$Pu	alpha to $^{234}_{92}$U	87.74	560	2600
$^{239}_{94}$Pu	alpha to $^{235}_{92}$U	24,100	1.9	0.022
$^{240}_{94}$Pu	alpha to $^{236}_{92}$U+ Spont. Fission	6560	6.8	910
$^{241}_{94}$Pu	e^- to $^{241}_{95}$Am	14.4	4.2	0.049
$^{242}_{94}$Pu	alpha to $^{238}_{92}$U	376,000	0.1	1700

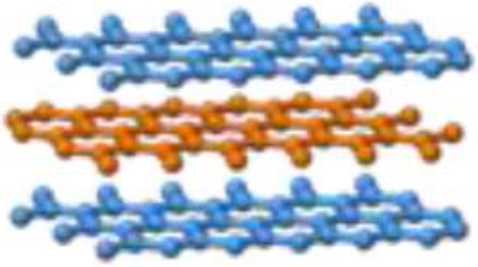

Figure 1. Side view of layer stacking of graphite (after Wikipedia).

2.3. Nuclear transmutation in hydrogen graphite HC_x ($x = 6$–8?)

We may then have a superlattice made of a carbon sublattice of graphite (Fig. 1) and a hydrogen sublattice occluded between carbon layers in the graphite. The HC_x superlattice may have a structure similar to the superlattice CaC_6 shown in Fig. 2. If the hydrogen graphite HC_x forms such a superlattice considered above, it forms the CF-matter which participates in the CFP by the mechanism proposed in our books ([2,7], Section 3.7) and [6,22]. Thus, the product elements observed in the system of carbon arc in water are explained by our TNCF model as a result of the nuclear transmutation catalyzed by the trapped neutrons ([3], Section 3.7). The product elements observed in carbon arcs include the following elements in addition to the most abundant iron (Fe); Si, S, Cl, K, Ca, Ti, Cr, Mn, Co, Ni,

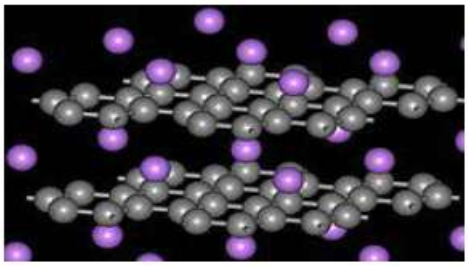

Figure 2. Structure of CaC_6: violet spheres represent Ca nuclei between layers of carbon nuclei (grey spheres) (after Wikipedia). We may imagine the structure of hydrogen graphite HC_x ($x = 6$ to 8 ?) which is not determined yet referring to this structure of CaC_6.

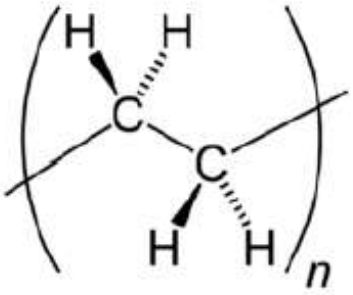

(a)

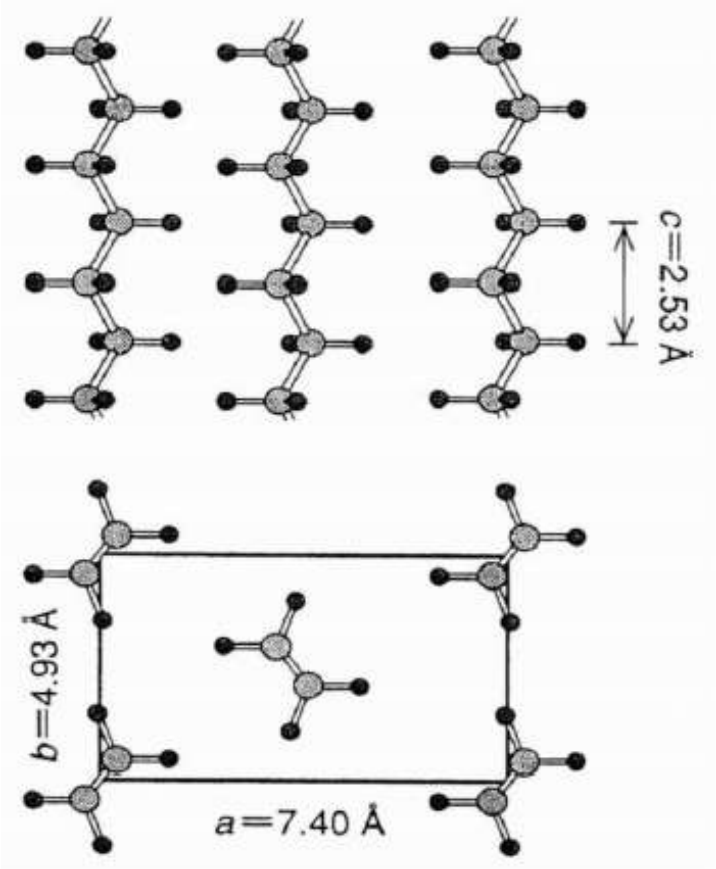

(b)

Figure 3. (a) Unit of polyethylene $(C_2H_4)_n$ ($n = \infty$). (b) Lattice structure of XLPE orthorhombic lattice with attice constants, $a = 7.40$ (740 pm), $b = 4.93$ (493 pm) and $c = 2.53$ (253 m) ([23], Fig. 5).

Cu, Zn and possibly heavier elements [3].

2.4. Nuclear transmutation in XLPE

Similarly, we can contemplate the appearance of neutron bands in XLPE shown in Fig. 3 [23]. The rather regular structure of the carbon–hydrogen array in XLPE suggests a similar mechanism to form the neutron bands as discussed in our recent papers [22,23]. The atomic arrays in biological cells are more complex than those of XLPE, as explained in Section 3, but we may be able to use the same idea used in the CFP general in biological systems.

Then, we can explain the nuclear transmutations in XLPE observed by the excellent experiments performed by Kumazawa et al. for more than 10 years starting in 2005, described in our papers [22,23]. For the illustration of nuclear transmutations in their systems including XLPE, see Table 3 from our paper [23], Table 2).

Table 3. Increase (+) and decrease (–) of inorganic elements in samples after voltage application (Table 2 of [23]).

Element	Isotopes	Sample		
		Dipped in KCl solution	Dipped in NaCl solution	Dipped in $AgNO_3$ solution
$_{3}$Li	^{6}Li, ^{7}Li			+
$_{11}$Na	^{23}Na		−	(+)
$_{12}$Mg	^{24}Mg, ^{25}Mg, ^{26}Mg		−	
$_{13}$Al	^{27}Al		+	
$_{19}$K	^{39}K, ^{40}K, ^{41}K	−		
$_{20}$Ca	^{40}Ca, ^{42}Ca, ^{43}Ca, ^{44}Ca, ^{46}Ca, ^{48}Ca	+		
$_{26}$Fe	^{54}Fe, ^{56}Fe, ^{57}Fe, ^{58}Fe			−
$_{28}$Ni	^{58}Ni, ^{60}Ni, ^{61}Ni, ^{62}Ni, ^{64}Ni			+
$_{47}$Ag	^{107}Ag, ^{109}Ag			(−)
$_{82}$Pb	^{204}Pb, ^{206}Pb, ^{207}Pb, ^{208}Pb			+
$_{83}$Bi	^{209}Bi			+

3. Characteristics of Biotransmutation

Applying the TNCF model to the problems of biotransmutation, we can use following reactions between a trapped neutron n and a nucleus ${}^{A}_{Z}X$ at or in the surface of a bacterium or a tissue [24]:

$$ {}^{A}_{Z}X + n \rightarrow {}^{A+1}_{Z}X^{*}. \tag{4} $$

In this reaction formula, ${}^{A+1}_{Z}X*$ is an excited state of the nucleus ${}^{A+1}_{Z}X$ which will decay through following several channels in free space:

$$ {}^{A+1}_{Z}X^{*} \rightarrow {}^{A+1}_{Z}X + \gamma, \tag{5} $$

$$ \rightarrow {}^{A+1}_{Z+1}Y + \mathrm{e}^{-} + \underline{\nu}_{\mathrm{e}}, \tag{6} $$

$$ \rightarrow {}^{A+1}_{Z-1}Y' - \mathrm{e}^{-}, \tag{7} $$

$$ \rightarrow {}^{A-4}_{Z-2}Y'' + {}^{4}_{2}\mathrm{He}, \tag{8} $$

where ν_{e} is an anti-particle of the electron neutrino, γ is a photon (in free space) and Y, $Y'a$nd Y'' are daughter nuclides of the reactions. In the CF materials, the *photon* γ in the free space is supposed to be absorbed by the CF-matter formed of neutrons in the neutron band and its energy dissipates in *phonons* to heat the system as a whole ([7], Section 3.7.5).

3.1. Recent experimental data on the biotransmutation obtained by Vysotskii et al. [25,26]

Vysotskii and his collaborators have performed sophisticated experiments and obtained refined data sets in biological systems over the last 20 years, mainly by as cited in our paper [24]. To bring about the complex structure of microorganisms and microbial cultures used in their experiments, we produce their fundamental structures shown in Fig. 4. The structure of cell walls in microbial cultures depicted in Fig. 4(c) show complex but similar regular structures to that in XLPE shown in Fig. 3.

There are data sets showing (1) production of ${}^{57}_{26}$Fe from ${}^{55}_{25}$Mn and also (2) acceleration of the decay of radioactive nucleus ${}^{157}_{55}$Cs, ${}^{140}_{56}$Ba and ${}^{140}_{57}$La in several bacterial cultures.

Experiments were conducted using several bacterial cultures (*Bacillus subtilis GSY 228, Escherichia coli K-1, Deinococcus radiodurans M–1*) as well as the yeast culture *Saccharomyces cerevisiae T–8*. Selection of these cultures was motivated either by their experimentally proven ability to grow in the heavy water based media, or by the prospect of using the radiation-stable culture *Deinococcus radiodurans M–1* in transmutation processes given the presence of powerful radioactive fields, as was noted earlier [26].

3.1.1. *Production of ${}^{57}_{26}$Fe in a CF material containing ${}^{55}_{25}$Mn*

An example of transmutation is the production of ${}^{57}_{26}$Fe in a CF material containing ${}^{55}_{25}$Mn. The nuclear reaction responsible to this case is suggested by Eqs. (5) and (6). We can explain the production of ${}^{57}_{26}$Fe from ${}^{55}_{25}$Mn by the following reactions based on the TNCF model [24], Section 3.1):

$$ {}^{55}_{25}\mathrm{Mn} + \mathrm{n} \rightarrow {}^{56}_{25}\mathrm{Mn}^{*} \qquad (\sigma = 13.41\ \mathrm{barn}), \tag{9} $$

$$ {}^{56}_{25}\mathrm{Mn}^{*} \rightarrow {}^{56}_{26}\mathrm{Fe} + \mathrm{e}^{-} + \underline{\nu}_{\mathrm{e}} \qquad (\tau = 2.5785\ \mathrm{h}), \tag{10} $$

$$ {}^{56}_{26}\mathrm{Fe} + \mathrm{n} \rightarrow {}^{57}_{26}\mathrm{Fe} \qquad (\sigma = 2.5914\ \mathrm{barn}). \tag{11} $$

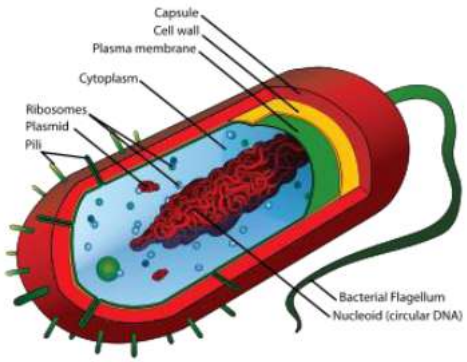

(a)

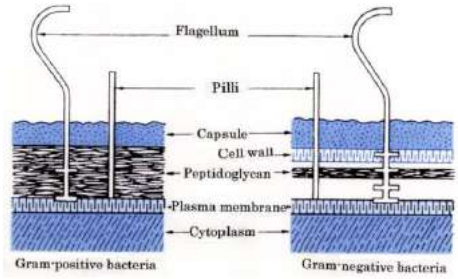

(b)

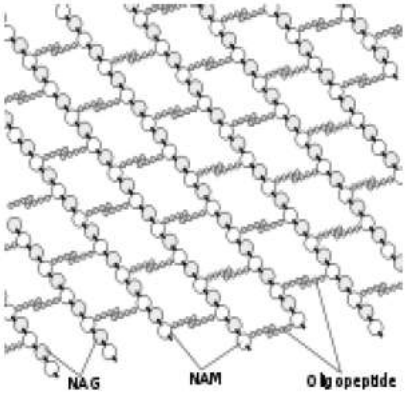

(c)

Figure 4. (a) Cell structure of a gram positive bacterium, (b) structures of cell walls in gram-positive and gram-negative bacteria and (c) structure of peptidoglycan (after Wikipedia).

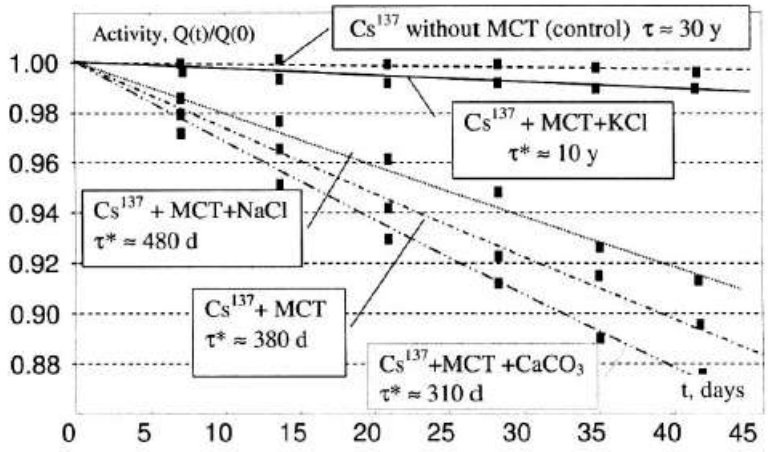

Figure 5. Accelerated deactivation (accelerated decay) of $^{137}_{55}$Cs isotope in "biological cells" with different chemical elements present ([25], Fig. 3.23, [26], Fig. 10). "MCT" in the explanation of this figure means the microbial transmutation catalyst, a special kind of granule.

3.1.2. *Decay-time shortening in biological system*

The observed acceleration of the decay process of $^{137}_{55}$Cs isotope is shown in Fig. 5. The behavior of the decay-time shortening in transition-metal hydrides had been noticed before and discussed in our paper already [13].

Another example of decay-time shortening in the biological system is obtained in $^{140}_{56}$Ba and $^{140}_{57}$La in pure reactor water with presence of metabolically active microorganisms as shown in Fig. 6.

3.2. Explanation of stabilization of unstable nuclei (or decay-time shortening) in biological system

The sophisticated experiments performed by Vysotskii et al. on the nuclear processes in biological systems revealed the existence of the decay-time shortening observed already in inorganic CF systems as discussed recently in our paper [24]. There are two examples of the decay-time shortening in biological system; one for $^{37}_{55}$Cs in electrolytic liquid, microbial catalyst-transmutator (MCT) + electrolyte (KCl, NaCl, or $CaCO_3$), and another for $^{140}_{56}$Ba and $^{140}_{57}$La in electrolytic liquid (water + metabolically active microorganisms). An explanation of MCT used in the experiment is given elsewhere [24].

3.2.1. $^{37}_{55}Cs$

The second example is the decay-time shortening of radioactive isotope $^{137}_{55}$Cs which decays in free space according to the following reaction shown in Fig. 5:

$$^{137}_{55}\mathrm{Cs} \rightarrow ^{137}_{56}\mathrm{Ba} + \mathrm{e}^- + \underline{\nu_\mathrm{e}} \qquad (\tau = 30.07 \text{ years}). \tag{12}$$

Assuming the existence of the trapped neutron in the TNCF model, we can apply Eq. (6) to this case:

$$^{137}_{55}\mathrm{Cs} + \mathrm{n} \rightarrow ^{138}_{55}\mathrm{Cs}^* \qquad (\sigma = 0.113 \text{ barn}), \tag{13}$$

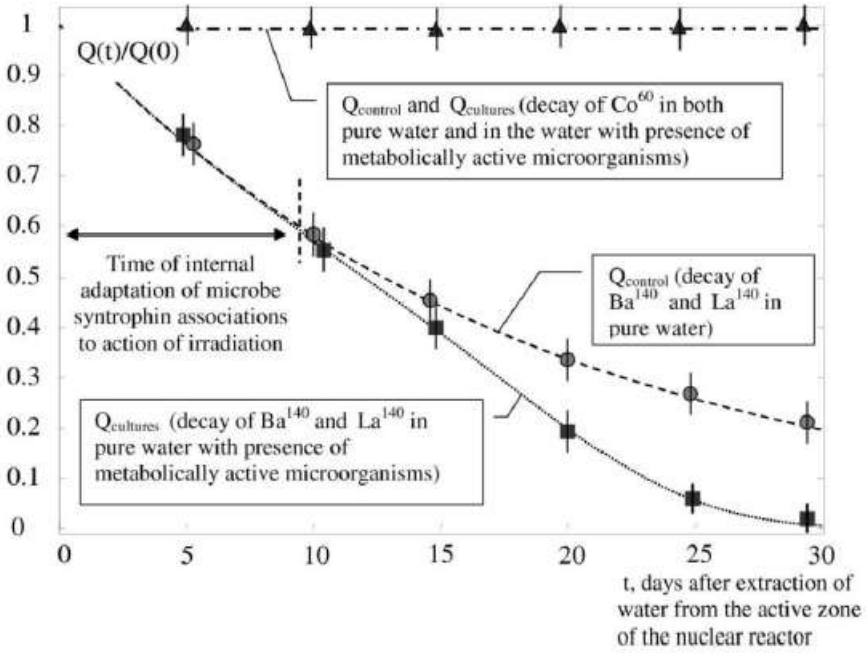

Figure 6. Change of activity Q(t) of the same reactor isotopes $^{140}_{56}$Ba, $^{140}_{57}$La and $^{60}_{27}$Co in the experiment on transmutation (activity Q_{cultures} in pure reactor water with presence of metabolically active microorganisms) and in the control one (activity Q_{control} in the same pure reactor water without microorganisms) ([25], Fig. 3.21, [26], Fig. 8).

$$^{138}_{55}\mathrm{Cs}^{*} \rightarrow ^{138}_{56}\mathrm{Ba} + \mathrm{e}^{-} + \underline{\nu_{\mathrm{e}}} \qquad (\tau = 33.41\ \mathrm{min}). \tag{14}$$

The difference of the effect of MCT + electrolyte (KCl, NaCl, or $CaCO_3$) on the decay-time shortening may reflect (1) a difference of the density of the trapped neutrons n_{n} or (2) a difference of the number of $^{137}_{55}$Cs nuclei on the MCT surface in the system due to the effect of electrolytic liquids (MCT + electrolytes) on the MCT.

The difference of measured decay times $\tau^{*} = 380$ days (MCT), 10 years (MCT + KCl), 480 days (MCT + NaCl), and 310 days (MCT + $CaCO_3$) compared to the natural decay time 30.1 years of $^{137}_{55}$Cs in free state shows the effect of the electrolytes on MCT where $^{137}_{55}$Cs nuclei are adsorbed and their decay characteristics are drastically influenced by the density of the trapped neutron in samples from our point of view. Thus, the electrolyte seems to have large effect on the adsorption characteristics of $^{137}_{55}$Cs by MCT.

This fact reminds us of the effect of K and Li on the CFP in Ni and Pd, which was discussed by us for many years ([28], Section 4, [7], Section 2.2.1.2).

"*It should be emphasized here that there is a preference for a combination of cathode metals (Pd, Ni, Ti, - -), an electrolyte (Li, Na, K, or Rb) and a solvent (D_2O or H_2O) to induce CFP.*" ([28], p. 45).

Let us investigate the characteristics of the decay-time shortening of $^{137}_{55}$Cs in these systems.

The temporal evolution of the number of a radioactive nuclide with a decay constant τ is described by following equations:

$$N(t) = N(0)\exp(-t/\tau), \tag{15}$$

$$\mathrm{d}N/\mathrm{d}t = -(N(0)/\tau)\exp(-t/\tau). \tag{16}$$

On the other hand, a decrease of the number of a nucleus ${}^{A}_{Z}X$ due to absorption of thermal neutrons described by Eq. (17) and relation (18) assumed in our model [5], Section 11.1), [7], Section 3.2):

$${}^{A}_{Z}X + \mathrm{n} = {}^{A}_{Z}X^{*} = {}^{A+1}_{Z}X + \text{phonons}, \tag{17}$$

$$P = \delta N_X/N_{\mathrm{X}} = 0.35\, n_{\mathrm{n}}\, v_{\mathrm{n}}\, \sigma_{\mathrm{nX}}. \tag{18}$$

In the above equations, n_{n} is the density of the trapped neutron, v_{n} is the thermal velocity of the assumed trapped neutron, N_X is the number of the nucleus ${}^{\mathrm{A}}_{Z}X$, and $\sigma_{\mathrm{n}X}$ is the absorption cross section of thermal neutrons by the nucleus X by reaction (17) ($\sigma_{\mathrm{nX}} = 0.113$ barn for ${}^{137}_{55}$Cs) assumed to be the same as the thermal neutron absorption cross section in free space. We use a value 2.2×10^5 cm/s for v_{n} according to our premises of the TNCF model.

If an ${}^{137}_{55}$Cs nucleus is adsorbed by the MCT granules to be reacted by the trapped neutron, reaction (17) is written down as

$${}^{137}_{55}\mathrm{Cs} + \mathrm{n} = {}^{138}_{55}\mathrm{Cs}^{*} = {}^{138}_{55}\mathrm{Cs} + \text{phonons}. \tag{19}$$

The reaction occurs with a probability P in a unit time interval for a nucleus ${}^{137}_{55}$Cs as expressed in Eq. (18):

$$P = \delta N_{\mathrm{Cs}}/N_{\mathrm{Cs}} = 0.35\, n_{\mathrm{n}}\, v_{\mathrm{n}}\, \sigma_{\mathrm{nCs}}. \tag{20}$$

Let us determine the density n_{n} of the TNCF model, assuming that the observed decay-time shortenings of ${}^{137}_{55}$Cs in electrolytic liquids depicted in Fig. 5 are the results of the neutron absorption described by Eq. (19).

As an example of our calculation, we take up the case of ${}^{137}_{55}$Cs in an electrolytic liquid with MCT + $CaCO_3$, where the observed decay time is $\tau^* = 310$ days. Using Eq. (16), we obtain the relative number of decayed nucleus in a unit time (1 day, for instance) as

$$\begin{aligned}\delta N/N &= -(1/\tau^*)\exp(-t/\tau^*)\\ &= -1/(310 \times 8.64 \times 10^4) = -1/2.68 \times 10^7\\ &= 3.73 \times 10^{-8}.\end{aligned} \tag{21}$$

In this calculation, note that the exponential factor exp (– t/τ^*) ≈ 1 and does not substantially contribute to the final result.

On the other hand, Eq. (20) gives n_{n} through the relative number of transmuted ${}^{137}_{55}$Cs nuclei $\delta N/N$ as:

$$\begin{aligned}n_{\mathrm{n}} &= (\delta N/N)/(0.35 \times 2.2 \times 10^5 \times 0.113 \times 10^{-24}) \times 1(s)\\ &= (\delta N/N)/(0.35 \times 2.2 \times 0.113 \times 10^{-19})\\ &= 1.15 \times 10^{19}(\delta N/N).\end{aligned} \tag{22}$$

Using the value of $\delta N/N$given in Eq. (21), we obtain the value of $n_{\rm n}$ in this case as

$$\begin{aligned} n_{\rm n} &= (\delta N/N)/(0.35 \times 2.2 \times 10^5 \times 0.113 \times 10^{-24}) \times 1(s) \\ &= (\delta N/N)/(0.35 \times 2.2 \times 0.113 \times 10^{-19}) \\ &= 1.15 \times 10^{19}(\delta N/N). \end{aligned} \tag{23}$$

If the number of $^{137}_{55}$Cs adsorbed by MCT granules and that not adsorbed are in the ratio $x : (1 - x)$, the calculation should be generalized to take into this fact. In the short time (e.g. 1 day) we are interested in, the number N_0 of $^{137}_{55}$Cs nuclei not adsorbed and therefore not influenced by the trapped neutron keeps its number $(1 - x)N_0$ almost the same as before (for the very long decay time of $\tau_0 = 30.1$ years):

$$\delta N/N|_1 = 0. \tag{24}$$

On the other hand, the nuclei adsorbed by MCT granules will suffer the action of the trapped neutron and its number xN_0 changes according to Eq. (20):

$$\delta N/N|_2 = 0.35\, n_{\rm n} v_{\rm n} \sigma_{\rm nM}. \tag{25}$$

Therefore, we have the change δN_0 of the number N_0 of $^{137}_{55}$Cs nuclei after the time interval t (= 1 day) given by $\delta N|_1$ due to the decay process (16) with $\tau = 30.1$ years and by $\delta N|_2$ due to the neutron trapping (20). Using relations (24) and (25), we obtain finally the expression for δN_0 /N_0 as given in Eq. (27):

$$\delta N_0 = \delta N|_1 + \delta N|_2 = \delta(1 - x)N_0|_1 + \delta x N_0|_2, \tag{26}$$

$$\delta N_0/N_0 = x(\delta N_0|_2/N_0) = x(0.35 n_{\rm n} v_{\rm n} \sigma_{\rm nM}). \tag{27}$$

Substituting the values $v_{\rm n} = 2.2 \times 10^5$ cm/s and $\sigma_{\rm nM} = 0.113$ barn, we obtain following equation:

$$\delta N_0/N_0 = x n_{\rm n}(0.35 \times 2.2 \times 10^5 \times 0.113 \times 10^{-24}) = 8.7 \times 10^{-21} x n_{\rm n}. \tag{28}$$

Therefore, the value $n_{\rm n}$ in this case is expressed as

$$n_{\rm n} = 1.15 \times 10^{19}(\delta N/N)x^{-1}({\rm cm}^{-3}). \tag{29}$$

If $x = 1$, i.e. all the $^{137}_{55}$Cs nuclei are adsorbed by MCT granules and influenced by the trapped neutron by Eq. (19), $\delta N/N = 3.73 \times 10^{-8}$ (21) gives the same value given in (23):

$$n_{\rm n} = 1.15 \times 10^{19}(\delta N/N)x^{-1} = 4.29 \times 10^{11}({\rm cm}^{-3}). \tag{30}$$

This value is compared with the values 10^7 – 10^{12} cm^{-3} obtained in inorganic CF materials given in our previous books ([5], Tables 11.2 and 11.3, [7], Tables 2.2 and 2.3).

As Eq. (16) (or Eq. (21)) shows that the decrease of the number of radioactive nuclei is proportional to the decay time τ* inversely and it is also proportional to x and $n_{\rm n}$ as shown in Eq. (27) (where x is the ratio of adsorbed nuclei). The differences of τ* observed in different electrolytic liquids are explained as follows.

If the density of trapped neutrons $n_{\rm n}$ is not influenced by the kind of electrolyte in the liquid, the difference of τ* depends only on the value of x which may depend on the electrolyte. The values of $\tau* = 310$, 380, 480 days, 10 years in the liquid with $CaCO_3$, non, NaCl, KCl, respectively, show that the ratios x in these electrolytic liquids are given by 1, 0.8, 0.6, 8.5 $\times 10^{-3}$, respectively taking the case of $CaCO_3$ as $x = 1$.

This result may show the aqueous solution of MCT granules is very effective at adsorbing a $^{137}_{55}$Cs nucleus (and change the value of x) and addition of $CaCO_3$ works positively but that of NaCl and KCl negatively to the adsorption, if our interpretation by the TNCF model of the decay-time shortening in the electrolytic liquids is right.

3.3. $^{140}_{56}$Ba and $^{140}_{57}$La

Similarly, we can analyze the cases of $^{140}_{56}$Ba and $^{140}_{57}$La shown in Fig. 6. The decay rates of these nuclides are described by the following formulae:

$$^{140}_{56}\mathrm{Ba} \rightarrow {}^{140}_{57}\mathrm{La} + \mathrm{e}^- + \underline{\nu_{\rm e}} \qquad (\tau = 12.752 \text{ days}), \tag{31}$$

$$^{140}_{57}\mathrm{La} \rightarrow {}^{140}_{58}\mathrm{Ce} + \mathrm{e}^- + \underline{\nu_{\rm e}} \qquad (\tau = 1.6781 \text{ days}). \tag{32}$$

The decay-time shortening of these nuclides is explained by the absorption of a neutron by $^{140}_{56}$Ba and $^{140}_{57}$La, followed by the beta-decay of the intermediate nuclei as shown:

$$^{140}_{56}\mathrm{Ba} + \mathrm{n} \rightarrow {}^{141}_{56}\mathrm{Ba}^* \qquad (\sigma = 1.63 \text{ barn}, \tag{33}$$

$$^{141}_{56}\mathrm{Ba}^* \rightarrow {}^{141}_{57}\mathrm{La} + \mathrm{e}^- + \underline{\nu_{\rm e}} \qquad (\tau = 18.27 \text{ min}) \tag{34}$$

and

$$^{140}_{57}\mathrm{La} + \mathrm{n} \rightarrow {}^{141}_{56}\mathrm{La}^* \qquad (\sigma = 2.73 \text{ barn}, \tag{35}$$

$$^{141}_{56}\mathrm{La}^* \rightarrow {}^{141}_{58}\mathrm{Ce} + \mathrm{e}^- + \underline{\nu_{\rm e}} \qquad (\tau = 3.92 \text{ h}). \tag{36}$$

On the other hand, the decay of $^{60}_{27}$Co is n intensified measurably by the existence and absorption of the trapped neutrons as shown by following equations:

$$^{60}_{27}\mathrm{Co} \rightarrow {}^{60}_{58} + \mathrm{e}^- + \underline{\nu_{\rm e}} \qquad (\tau = 10.47 \text{ min}), \tag{37}$$

$$^{60}_{27}\mathrm{Co} + \mathrm{n} \rightarrow {}^{61}_{27}\mathrm{Co}^* \qquad (\sigma = 2.02 \text{ barn}), \tag{38}$$

$$^{61}_{27}\mathrm{Co}^* \rightarrow {}^{61}_{58}\mathrm{Ni} + \mathrm{e}^- + \underline{\nu_{\rm e}} \qquad (\tau = 1.65 \text{ h}). \tag{39}$$

Thus, the experimental data sets obtained for $^{140}_{56}$Ba, $^{140}_{57}$La and $^{60}_{27}$Co shown in Fig. 6 are consistently explained by the TNCF model.

3.4. Other biotransmutations

Regarding the data on biotransmutations, some examples have been known since 18th century. Here are some quotes relating to our investigation, from page 25 of Michio Kushi's book [9]. The elemental transmutation (ET) in biological systems is considered as "most likely taking place at the cellular level."

"- - - it was concluded that, granted the existence of transmutations (Na to Mg, K to Ca, Mn to Fe), then a net surplus of energy was also produced."

"A proposed mechanism was described in which Mg adenosine triphosphate (MgATP) played a double role as an energy producer." "The MgATP, when placed in layers one atop the other, has all the attributes of a cyclotron."

"It was concluded that elemental transmutations were indeed occurring in life organs and were probably accompanied by a net energy gain." ([9], p. 25)

This summary of the biotransmutations by M. Kushi is based on many observations by Vauquelin and others which are introduced in our book ([5], Section 10.1, Biotransmutation).

3.5. Characteristics of biotransmutations applicable to the remediation of the hazardous nuclear waste

In inorganic systems used in CFP, it is known that there are specific favorable combinations of an electrode and an electrolyte to produce CFP in electrolytic experiments: Pd–Li and Ni–K are the most outstanding pairs used in positive experiments [27].

It might be possible to have a biological system in which the CF material (e.g. a bacterium) selectively adsorbs a specific element on the surface, depending on the nature of the surface or of the material. Then if the bacterium works as an agent similar to the MCT in Fig. 5, the system might effectively remediate hazardous radioactive waste.

4. Quantum Mechanical Bases of the Neutron Drop Model

It has been shown that our phenomenological approach by the TNCF model with an adjustable parameter (and by the neutron drop model) gives a consistent and unified explanation of almost all experimental results obtained in the CFP not only for deuterides but also for hydrides. Furthermore, we explained the CFP observed in hydrogen graphite and biological systems by the TNCF model.

We give a brief explanation of the TNCF and the ND models and explain quantum mechanical bases of these models.

4.1. TNCF model and neutron drop model

The original TNCF model was proposed in 1993 at ICCF4. It assumes the existence of quasi-stable neutrons in CF materials [4].

4.1.1. *A phenomenological approach to the CFP – the TNCF model and the neutron drop model*

We have proposed a unified explanation of various experimental data sets by the TNCF model introduced at ICCF4, and we published a book containing the results of analyses in 1998 [5]. In the original model, we assumed nuclear reactions induced by absorption of single neutron by a nucleus in the system. It was remarkable to note that the model could explain observed data of several quantities in an experiment consistently using only one adjustable parameter.

To explain the nuclear transmutations with large changes of proton and neutron numbers, we extended the TNCF model to the ND (neutron drop) model in which we assumed existence of neutron drops ${}^{A}_{Z}\Delta$ composed of $(A - Z)$

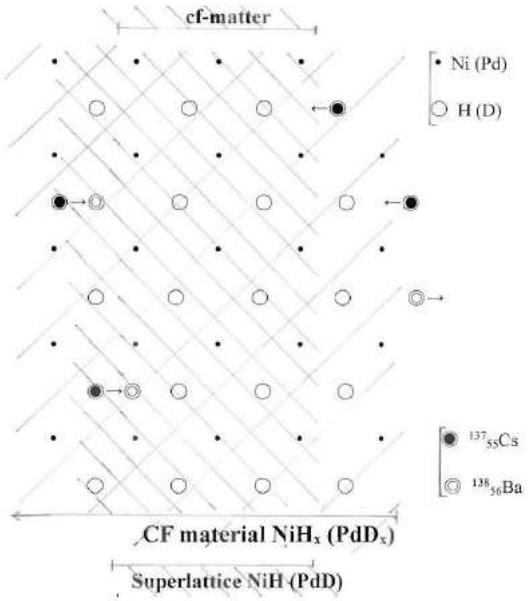

Figure 7. Schematic explanation of nuclear transmutations at the surface region of a CF material (e.g. NiH_x (PdD_x) in this figure). The nuclear transmutation explained in Section 3.2 (Eqs. (13) and (14)) is illustrated in this figure.

neutrons and Z protons suggested by the neutron star matter [18]. We named the state with neutron drops "CF-matter" for convenience in future discussions [7].

We have investigated the basis of trapped neutrons and neutron drops in such CF materials as transition metal deuterides and hydrides, using quantum mechanics on the interaction of host elements and hydrogen isotopes [6,7]. The schematic explanation of the CF material (e.g. NiH_x) at its surface region is shown in Fig. 7.

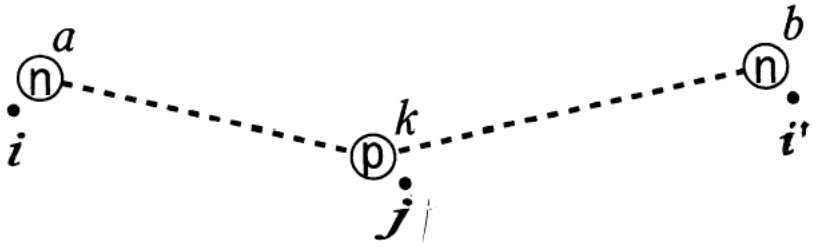

Figure 8. The super-nuclear interaction between two neutrons a and b in lattice nuclei $\boldsymbol{i}$ and $\boldsymbol{i}$' mediated by a proton (or a deuteron) k at an adjacent interstitial site $\boldsymbol{j}$ ([7], Fig. 3.3).

4.1.2. *Super-nuclear interaction of neutrons at lattice nuclei mediated by interstitial protons or deuterons*

The nuclear interaction between an interstitial proton (or deuteron) and a nucleus of the host elements on a lattice point (a lattice nucleus) induces the super-nuclear interaction between neutrons in different lattice nuclei when the interstitial proton (or deuteron) has an extended wavefunction reaching the lattice points as shown in Fig. 8 [7].

4.1.3. *Formation of the neutron bands and the CF-matter at boundary region*

The super-nuclear interaction results in the neutron bands and finally the CF-matter. The superlattice of the host elements and the hydrogen isotopes is an optimum structure to produce CF-matter [28].

The neutron waves in a neutron band are reflected at the boundary of the CF material and accumulate there as shown in Fig. 9.

The high density neutrons so created at the boundary region behave the same way as neutron star matter [18] and form the CF-matter ([7], Section 3.7.5). In the CF-matter, neutron drops ${}^{A}_{Z}\Delta$ may exist, as shown by the simulation for the neutron star matter [18].

4.1.4. *De-excitation of unstable nuclei by the interaction among particles in the CF-matter*

The mutual interactions among particles in CF-matter induces the de-excitation of lattice nuclei ${}^{A}_{Z}\mathrm{Y}^{*}$ at an excited state resulting in elevation of energies of the CF-matter ([7], Section 3.7.6). Finally, the elevated energy of the CF-matter is dissipated to lattice energy of the CF material, as explained below

4.1.5. *Neutron–phonon Interaction in CF-matter*

The neutron–neutron interaction mediated by interstitial protons or deuterons depends on the lattice sites $\boldsymbol{R}_{\mathrm{i}}$ of the relevant lattice nuclei. We have worked out the interaction formulae for the super-nuclear interaction at absolute zero where the lattice of host elements is at rest ([7], Sectin 3.7.1). The displacement of a nucleus ${}^{A}_{Z}\mathrm{X}$ at a lattice site $\boldsymbol{R}_{\mathrm{i}}$ by

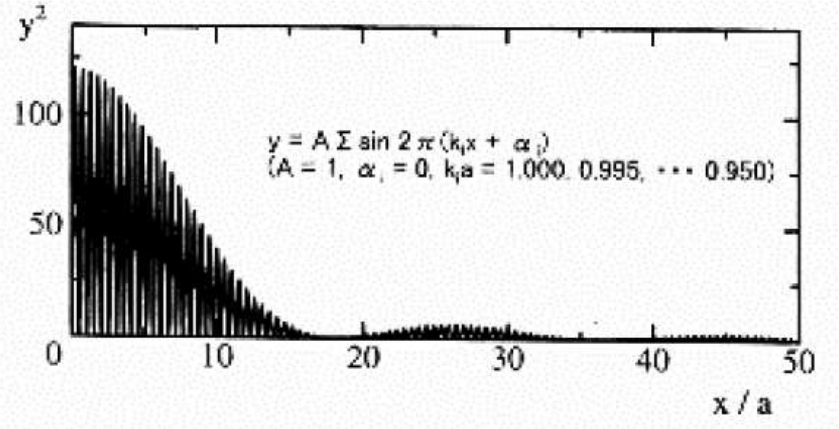

Figure 9. Neutron density accumulation of 11 neutrons reflected coherently at boundary. Abscissa is the distance in a unit of lattice constant $a$from the boundary where the neutron waves reflected. When a wave is reflected, the profile is a straight line at a height one parallel to the abscissa ([7], Fig. 3.4).

the lattice vibration at a finite temperature induces an interaction of neutrons in the neutron band and phonons of the lattice vibration.

This neutron–phonon interaction is responsible for the dissipation of neutron energy increased by the de-excitation of lattice nuclei. Thus, the emission of photons when the excited nuclei are de-excited in free space is alternatively resolved by the emission of phonons, as explained above. This mechanism explains the stabilization of unstable nuclei in the CF materials without emission of photons expected in free space.

4.2. Surface nature of nuclear reactions in the CFP

A superlattice of PdD is apt to be formed by self-organization at the surface region where the density of D is higher [28]. The super-nuclear interaction between neutrons results in the neutron bands and finally formation of CF-matter at boundary regions. The neutron drops $AZ\Delta$ in the CF-matter participate in the nuclear transmutations of foreign nuclei at the surface region as shown in Fig. 7 [7,28].

4.3. Non-linear dynamics and complexity in the CFP

The qualitative reproducibility and other characteristics of the CFP pointed out in the Introduction of this paper suggests that the complexity investigated extensively in the non-linear dynamics in recent years has close relation with physics of atoms and atomic nuclei in the CF materials. The three laws found in the CFP should have also close relation with the complexity in the CFP [29].

The three laws are as follows:

(1) The First Law: the stability effect for nuclear transmutation products.
(2) Second Law; the inverse power dependence of the frequency on the intensity of the excess heat production.
(3) Third Law: bifurcation of the intensity of events (neutron emission and excess heat production) in time.

We see that the second and the third laws have especially close connection with complexity. We investigated the relationship of complexity with the CFP in previous papers [28,30].

4.4. Inductive logic and meta-analysis in the CFP

Since the development of modern science in 16th century, physics developed according to the deductive logic guided by fundamental principles that govern simple systems following linear dynamics. The natural history used widely in science before the rise of modern science had been put aside as old-fashioned thinking.

However, we have to reconsider the logic useful in the investigation of nature. In nature, non-linear interactions are ubiquitous and therefore complexity prevails, as revealed by non-linear dynamics. Inductive logic should be effective to investigate phenomena occurring in complicated systems governed by non-linear interactions [31].

K. Nakamura, a molecular biologist, expressed her credo on the bio-history (natural history in biology) [32] leaving reductionism (based on the deductive logic) prevailed in the natural science since the beginning of the modern science in 17th century as follows:

"The history in Bio-history means a tale of history. I wanted to spin a story about the diverse nature based on the life. It was my object of research at present. In modern science, we have spent our time advancing toward a truth, and we have to write papers on results obtained independent of history. However, science is changing now. The time of exoscience, i.e. the science where the researcher is outside the objective system and describes the phenomena logically, objectively and universally, has gone. The so-called endoscience, i.e. the science where the researcher is in the system, is being born. Bio-history does not forbid modern science from going another way, but faithfully takes just its extended

way further. It seems to me that the science itself, including physics, is moving into endoscience now, in parallel to the transition of 'the time of reason' to 'the time of life'." ([32], p. 218)

It should also be noted that analysis of experimental data should be reconsidered in view of the history of science. The meta-analysis is widely used in medical science where there is a great deal of data not reproducible exactly, while we meet reproducibility in physical science of linear dynamics [33,34]. The problem in medical science is the same as in our investigation of the data for CFP [5,7]. We have to reconsider our problem from the general point of view as will be presented in our future papers [31,35].

We cite here several sentences related to the definition and considerations on the meta-analysis.

The meta-analysis is defined as follows:

"It is possible to define the *Meta-Analysis as 'The analysis of the data for a research question where are plural trials*.' " ([33], p. 1418)

In short, the essential procedure of the meta-analysis, summarized by K. Tsutani as follows, suggests that our analysis of the data in the CFP in the last 30 years should be classified as this method even if it may have not done completely as the work of an individual:

"The Process of the Meta-Analysis ([34], pp. 1417–1418), Translated into English by H.K.)

There are seven steps in a meta-analysis:

(1) *Set the Research Theme, i.e. the Research Question.*
    In the first step "Identification of the Problem" of the EBM, the four elements called "PECO" (i.e. patient, exposure, comparison, and outcome) are about a specific patient. In the identification of the problem at the meta-analysis, the generalized "name of disease" corresponds to the patient in the PECO.
(2) *Collection of Research without Exception.*
    This is a very important step. We have to collect as many trials as possible including unpublished ones to avoid publication bias. Considering this point, it is very difficult to develop the systematic review at the individual level. It is desirable to have support by public organizations.
(3) Evaluation of Values of Individual Researches
(4) Summarization of the Result of the Evaluation
(5) Systematic Analysis of the Result
(6) Interpretation of the Result
(7) Edit and Publication of the Result periodically"

5. Conclusion

Nuclear reactions in the CFP, including nuclear transmutation, are wonderful phenomena difficult to understand with traditional solid-state physics and nuclear physics. The confusion in this field since the discovery of the cold fusion phenomenon in 1989 has shown the overwhelming influence of the deductive logic established in modern science since 17th century as seen in the history of the CFP [36].

To understand the complex experimental data obtained in the CFP consistently, we have to depend on the phenomenological approach with a model [4,5] as a kind of meta-analysis and then on the quantum mechanics to investigate the premises used in the model [7]. The model proposed in 1994 (TNCF model) successfully explained various events observed in the CFP. The consistent explanation of experimental facts by the model has shown the reality of the participation of neutrons in the nuclear reactions in the CF materials where the CFP has been observed. The quantum mechanical investigation of the nuclear interaction between lattice nuclei and interstitial protons or deuterons has given a new feature of the interaction between lattice nuclei in the CF materials [7].

It is valuable to point out the use of the meta-analysis in such complex situations as those met in the medical fields, where they call the analysis "EBM" (evidence based medicine) or "Systematic Review." The analysis of the data sets

in the CFP performed in our works [5,7] could be classified as a kind of the meta-analysis. In forthcoming papers [31,35], we will give an extensive investigation of the meta-analysis in the CF research. We also notice that the logic used in our explanation of the CFP by the TNCF model is classified into the inductive logic rather than the deductive one prevalently used in the modern science developed after 17th century. We will discuss these points extensively in these forthcoming papers.

We have explained several characteristics of the nuclear transmutations and the decay-time shortenings obtained in non-biological CF materials as follows:

(1) In electrolytic systems, the electrolyte elements (Li, K, and so on) adsorbed on the cathodes (Pd, Ni, and so on) have shown nuclear transmutations at the near surface layers to a depth of a few micrometers ([5], Section 11.11, [7], Section 2.5.1).
(2) In the case of actinoid hydrides and deuterides, co-deposited U_3O_8 and H on Ni cathode has shown the decay-time shortening of uranium [17].

In addition to these examples obtained in non-biological CF materials, there are nuclear transmutations and decay-time shortenings in biological systems as introduced in Section 3.

We must recognize the importance of the problem of how to treat nuclear waste that is piling up in our society. The patent issued recently for the "Method of Treatment of the Radioactive Waste" (in Japanese) [20] shows the urgency of such treatment.

We have given a consistent explanation for the nuclear reactions in various CF materials from the biotransmutation, i.e. nuclear transmutation in biological systems, to nuclear transmutations in other CF materials. If our explanation of the biotransmutation is correct, we can contemplate the application of this phenomenon to nuclear waste treatment as follows.

As the patent [20] shows clearly, the method based on the nuclear physics in free space is a rival to the treatment of radioactive waste by the CFP. The key factor in this competition is the cost-performance ratios of two methods. We have to check our technique in detail as soon as possible.

As we know from experimental results presented briefly in this paper, the nuclear reactions in the CFP occur at localized regions near boundaries of CF materials and the efficiency of the nuclear reactions is exceptionally higher than that occurs in free space. On the other hand, we need CF materials that have longevity. We may have many factors to check before realization of these new techniques. Anyway, competition is always desirable to improve techniques.

It is well known that some biological systems characteristically adsorb specific anion or cation selectively. These characteristics of the biological systems may enable us to use them effectively to remediate hazardous nuclear waste.

We can systematize the process of biotransmutation research as follows: First, find microorganisms that adsorb ions of specific elements. Second, find microorganisms that affect unstable nuclear states adsorbed on the surface. Third, determine the molecular structures of the microorganism that has shown the ability of nuclear transmutation. Using these three steps cyclically, we can make progress in the research of remediation of hazardous nuclear wastes by the biotransmutation.

It may be possible to imagine a fantastic dream to have some microorganisms that obtain their energy from unstable nuclei destabilizing them by the mechanism we had known in the biotransmutation summarized in this paper. Biological systems are a source of miracles we have had in past and will have in future.

Acknowledgement

The author would like to thank Mr. Jed Rothwell for his help in correcting the mistakes in English sentences and rectifying the misunderstanding of the content.

References

[1] M. Fleischmann, S. Pons and M. Hawkins, Electrochemically induced nuclear fusion of deuterium, *J. Electroanal. Chem*. **261** (1989) 301–308.

[2]] H. Kozima, Cold fusion phenomenon in open, nonequilibrium, multi-component systems, *Reports of CFRL* (*Cold Fusion Research Laboratory*) **12-1** (2012) 1–14. http://www.geocities.jp/hjrfq930/Papers/paperr/paperr.html.

[3] H. Kozima, From the history of CF research – A review of the typical papers on the cold fusion phenomenon, *Proc. JCF16* **16–13** (2016) 116–157. ISSN 2187-2260, http://jcfrs.org/proc_jcf.html.

[4] H. Kozima, Trapped neutron catalysed fusion of deuterons and protons in inhomogeneous solids, *Trans. Fusion Technol.* **26** (1994) 508–515. ISSN 0748-1896.

[5] H. Kozima, *Discovery of the Cold Fusion Phenomenon,* Ohtake Shuppan Inc., Tokyo, Japan, 1998. ISBN: 4-87186-044-2.

[6] H. Kozima, Cold fusion phenomenon, *Rep. Fac. Science, Shizuoka Univ*. **39** (2005) 21–90. ISSN 05830923.

[7] H. Kozima, *The Science of the Cold Fusion Phenomenon*, Elsevier, 2006. ISBN-10: 0-08-045110-1.

[8] U.S. Army Material Technology Laboratory, *Energy Development from Elemental Transmutations in Biological System*, 1978.

[9] M. Kushi, *The Philosopher's Stone*, One Peaceful World Press, 1994.

[10] H. Kozima, K. Hiroe, M. Nomura and M. Ohta, Elemental transmutation in biological and chemical systems, *Cold Fusion* **16** (1996) 30–32, ISSN 1074-5610,
http://www.geocities.jp/hjrfq930/Papers/paperc/paperc.html.

[11] V.I. Vysotskii, A.A. Kornikova and I.I. Samoylenko, Experimental discovery of the phenomenon of low-energy nuclear transmutation of isotopes (^{55}Mn $\rightarrow$ ^{57}Fe) in growing biological cultures, *Proc. ICCF6* (1996) , pp. 687–693.

[12] V.I. Vysotskii and A.A. Kornilova, Microbial transmutation of Cs-137 and LENR in growing biological systems, *Current Science* **108** (2015) 636–641 (Increasing decay rate of Cs-137 isotope**).**

[13] H. Kozima, Nuclear transmutations (NTs) in cold fusion phenomenon (CFP) and nuclear physics, *Proc. JCF14,* **14–15** (2014) 168–202. ISSN 2187-2260, http://jcfrs.org/proc_jcf.html. Also *Reports of CFRL* (*Cold Fusion Research Laboratory*) **14-3** (2014) 1–35.
http://www.geocities.jp/hjrfq930/Papers/paperr/paperr.html.

[14] G. Goddard, J. Dash and S. Frantz, Characterization of uranium co-deposited with hydrogen on nickel cathodes, *Trans. Am. Nucl. Soc*. **83** (2000) 376–378.

[15] J. Dash, I. Savvatimova, S. Frantz, E. Weis and H. Kozima, Effects of glow discharge with hydrogen isotope plasmas on radioactivity of uranium, *Proc. ICCF9*, 2003, pp. 77–81. ISBN 7-302-06489-X/O·292.

[16] J. Dash and D. Chicea, Changes in the radioactivity, topography, and surface composition of uranium after hydrogen loading by aqueous electrolysis, *Proc. ICCF10*, 2005, pp. 463–474. ISBN 981-256-564-7.

[17] H. Kozima, Nuclear transmutation in actinoid hydrides and deuterides**,** *Proc. JCF14* **14-6** (2014) 77–94. ISSN 2187-2260.
http://jcfrs.org/proc_jcf.html.

[18] J.W. Negele and D. Vautherin, Neutron star matter at sub-nuclear densities, *Nucl. Phys.* **A207** (1973) 298–320. ISSN: 0375-9474.

[19] H. Kozima and K. Kaki, Atomic nucleus and neutron – nuclear physics revisited with the viewpoint of the cold fusion phenomenon, *Proc. JCF14* **14-5** (2014) 47–76. ISSN 2187-2260.
http://jcfrs.org//proc_jcf.html. Also *Reports of CFRL* (*Cold Fusion Research Laboratory*) **14-1** (2014) 1–34. http://www.geocities.jp/hjrfq930/Papers/paperr/paperr.html.

[20] [JP Patent No. 6106892] JP 6106892 B2 2017.4.5.
https://jopss.jaea.go.jp/pdfdata/P2/P14027B.pdf.

[21] H. Kozima, *Quantum Physics of Cold Fusion Phenomenon, in Developments in Quantum Physics*, F. Columbus and V. Krasnoholovets (Eds.), Nova Science publishers, New York, 2004, ISBN 1-59454-003-9.

[22] H. Kozima, Nuclear transmutations in polyethylene (XLPE) films and water tree generation in them (2), *Proc. JCF16* **16-17** (2016) 210–215. ISSN 2187-2260. http://jcfrs.org/proc_jcf.html.

[23] H. Kozima and H. Date, Nuclear transmutations in polyethylene (XLPE) films and water tree generation in them, *Proc. ICCF14* (August 10-âĂŞ 15, 2008, Washington D.C., USA), pp. 618-âĂŞ622 (2010), ISBN 978-0-578-06694-3.

[24] H. Kozima, Biotransmutation as a cold fusion phenomenon, *Proc. JCF16,* **16-18** (2016) 216–239. ISSN 2187-2260. http://jcfrs.org/proc_jcf.html.
[25] V.I. Vysotskii and A.A. Kornilova, *Nuclear Transmutation of Stable and Radioactive Isotopes in Growing Biological Systems*, Pentagon Press, India, 2009.
[26] V.I. Vysotskii and A.A. Kornilova, Transmutation of stable isotopes and deactivation of radioactive waste, *Ann. Nucl. Energy* **62** (2013) 626-âĂŞ633.
[27] H. Kozima, Electroanalytical chemistry in cold fusion phenomenon, in Recent Research Developments in Electroanalytical Chemistry, S.G. Pandalai (Ed.), Transworld Research Network, 2000, pp. 35-âĂŞ46, ISBN 81-86486-94-8. This paper is posted at the CFRL website: http://www.geocities.jp/hjrfq930/Papers/papere/papere.html.
[28] H. Kozima, Cold fusion phenomenon in open, nonequilibrium, multi-component systems – self-organization of optimum structure, *Proc. JCF13* **13–19** (2013) 134–157. ISSN 2187-2260. http://jcfrs.org//proc_jcf.html.
[29] H. Kozima, Three laws in the cold fusion phenomenon and their physical meaning, *Proc. JCF12*, 2012, pp. 101–114. ISSN 2187-2260.
http://jcfrs.org//proc_jcf.html.
[30] H. Kozima, Complexity in the cold fusion phenomenon *Proc. ICCF14* 2010, pp. 613–617 ISBN 978-0-578-06694-3
[31] H. Kozima, Inductive logic and meta-analysis in the cold fusion phenomenon, *Proc. JCF19* (2019) (to be submitted).
[32] K. Nakamura, *Self-developing Life – A story of Universality and Individuality –*, Tetsugaku-shobo, Tokyo, Japan, 1993. ISBN 4-88679-055-0 (In Japanese).
[33] K. Tsutani, Examination of evidence in EBM, *Therapeutic Res.* **24** (8) (2003) 1415–1422.
[34] E. Walker, A.V. Hernandez and M.W. Kattan, Meta-analysis: its strengths and limitations, *Cleve. Clinic. J. Med.* **75** (6) (2008) 431–439. PMID 18595551.
[35] H. Kozima, Development of the solid state-nuclear physics, *Proc. JCF19* (2019) (to be submitted).
[36] H. Kozima, The sociology of the cold fusion phenomenon -âĂŞ An essay -âĂŞ, *Proc. JCF17* **17-13** (2017) 148–219, ISSN 2187-2260, http://jcfrs.org/proc_ jcf.html.